Cancer Cell
Article

The Requirement for Cyclin D Function in Tumor Maintenance

Yoon Jong Choi,[1,8,11] Xiaoyu Li,[2,9,11] Per Hydbring,[1,8] Takaomi Sanda,[3,7,10] Joanna Stefano,[1] Amanda L. Christie,[4] Sabina Signoretti,[5,6] A. Thomas Look,[3,7,10] Andrew L. Kung,[4,10,12] Harald von Boehmer,[2,9] and Piotr Sicinski[1,8,*]
[1]Department of Cancer Biology
[2]Department of Cancer Immunology and AIDS
[3]Department of Pediatric Oncology
[4]Lurie Family Imaging Center
[5]Department of Medical Oncology
Dana-Farber Cancer Institute, Boston, MA 02215, USA
[6]Department of Pathology, Brigham and Women's Hospital, Boston, MA 02115, USA
[7]Division of Hematology/Oncology, Children's Hospital, Boston, MA 02115, USA
[8]Department of Genetics
[9]Department of Microbiology and Immunology
[10]Department of Pediatrics
Harvard Medical School, Boston, MA 02115, USA
[11]These authors contributed equally to this work
[12]Present address: Division of Pediatric Hematology/Oncology/Stem Cell Transplantation, Columbia University Medical Center, New York, NY 10032, USA
*Correspondence: peter_sicinski@dfci.harvard.edu
http://dx.doi.org/10.1016/j.ccr.2012.09.015

SUMMARY

D-cyclins represent components of cell cycle machinery. To test the efficacy of targeting D-cyclins in cancer treatment, we engineered mouse strains that allow acute and global ablation of individual D-cyclins in a living animal. Ubiquitous shutdown of cyclin D1 or inhibition of cyclin D-associated kinase activity in mice bearing *ErbB2*-driven mammary carcinomas triggered tumor cell senescence, without compromising the animals' health. Ablation of cyclin D3 in mice bearing *Notch1*-driven T cell acute lymphoblastic leukemias (T-ALL) triggered tumor cell apoptosis. Such selective killing of leukemic cells can also be achieved by inhibiting cyclin D associated kinase activity in mouse and human T-ALL models. Inhibition of cyclin D-kinase activity represents a highly-selective anticancer strategy that specifically targets cancer cells without significantly affecting normal tissues.

INTRODUCTION

The proliferation of mammalian cells is driven by the core cell cycle machinery operating in the cell nucleus. The key components of this machinery are proteins called cyclins, which bind, activate, and provide substrate specificity to cyclin-dependent kinases (CDKs). Cyclin-CDK complexes phosphorylate cellular proteins, thereby driving cell cycle progression (Malumbres and Barbacid, 2009).

Among all cyclin classes, D-type cyclins are of particular importance to the cancer field, as they represent the ultimate recipients of many oncogenic pathways (Deshpande et al., 2005; Fu et al., 2004; Musgrove et al., 2011). This family is composed of cyclins D1, D2, and D3, which show substantial amino acid sequence similarity, and are expressed in an overlapping, redundant fashion in all proliferating cell types (Musgrove et al., 2011). D-cyclins bind and activate CDK4 and CDK6; cyclin D-CDK4 and D-CDK6 complexes phosphorylate

Significance

D-cyclins are recipients of many oncogenic signals, and are often overexpressed in human cancers. This study tests the consequences of an acute and global inhibition of D-cyclins in vivo, in a living mouse. We found that cyclins D1 or D3 are largely dispensable for normal physiology of adult animals, but they are essential for tumor maintenance. We demonstrated that acute cyclin D1- or D3-inhibition causes tumor cell senescence or apoptosis. Hence, therapeutic targeting of D-cyclins is expected to be highly specific in shutting off cancer progression, without significantly affecting normal tissues. Our demonstration that inhibition of cyclin D-CDK kinase selectively kills mouse and human leukemic cells in vivo suggests a potential therapeutic strategy in patients bearing these malignancies.

the retinoblastoma tumor suppressor protein, pRB, and pRB-like p107 and p130 proteins, leading to activation or derepression of E2F transcription factors. E2Fs then induce several target genes that are required for entry of cells into the DNA synthesis (S) phase (Trimarchi and Lees, 2002). In addition, cyclin D-CDK4 and D-CDK6 complexes play a second, noncatalytic function in G1 phase progression through sequestration of cell cycle inhibitors $p27^{Kip1}$ and $p21^{Cip1}$, which leads to activation of CDK2-containing complexes (Sherr and Roberts, 2004).

Amplification of individual cyclin D genes and overexpression of their encoded proteins were documented in a large proportion of human cancers. For example, cyclin D1 is overexpressed in the majority of breast cancer cases, whereas overexpression of cyclin D3 is observed in many lymphoid malignancies (Deshpande et al., 2005; Fu et al., 2004; Musgrove et al., 2011). A comprehensive analysis of many human cancer types revealed that the gene encoding cyclin D1 represents the second most frequently amplified locus in the human cancer genome (Beroukhim et al., 2010). Moreover, in many human cancers overexpression of D-type cyclins takes place in the absence of any detectable genomic alterations (Deshpande et al., 2005; Fu et al., 2004; Musgrove et al., 2011).

It was initially assumed that individual D-type cyclins are required for proliferation of normal, nontransformed cells. However, we and others found that knockout mice lacking individual D-cyclins are viable, and display only minor phenotypes, revealing that these proteins are dispensable for development of the overwhelming majority of organs (Sherr and Roberts, 2004). In contrast, particular D-cyclins were shown to be essential for tumor initiation in vivo in the specific compartments. For example, mice lacking cyclin D1 are resistant to *ErbB2*-driven mammary adenocarcinomas, while cyclin D3 null animals are refractory to *Notch1*-driven T-ALL (Bowe et al., 2002; Landis et al., 2006; Sicinska et al., 2003; Yu et al., 2001).

These analyses established an essential requirement for D-cyclins in tumor initiation. An important unresolved question is whether these proteins are also required for tumor maintenance, and whether their ablation in mice that already developed tumors would have an effect on tumor progression.

Another critical question for therapeutic targeting of D-cyclins is what would be the consequence of an acute shutdown of individual D-cyclins in the whole animal. Knockout mice lacking particular D-cyclins displayed only minor phenotypes, but these mice developed from the very beginning in the absence of a cyclin D-protein. It is well-established that "constitutive," germline knockout animals often activate compensatory mechanisms (Lin et al., 2008; Sage et al., 2003), whereas an acute shutdown of a protein in an adult animal may have much more profound consequences.

To address these questions, we developed mouse models that allowed us to inducibly shut off cyclin D function in the whole animal. Using these models, we acutely and ubiquitously ablated expression of cyclin D1 or D3 in adult mice that developed different types of tumors.

RESULTS

Acute Ablation of Cyclin D1 in Adult Mice

In order to determine the consequence of an acute and global ablation of cyclin D1 in adult mice, we generated conditional cyclin D1 knockout ($D1^{F/F}$) animals (Figures S1A–S1C available online). We determined that *cyclin* $D1^{F/F}$ mice developed normally and displayed no phenotypic abnormalities, consistent with the expectation that the "floxed" *cyclin D1* allele is functionally wild-type. We interbred *cyclin* $D1^{F/F}$ and *cyclin* $D1^{-/-}$ mice and generated heterozygous *cyclin* $D1^{F/-}$ animals that were used in the analyses described below. These *cyclin* $D1^{F/-}$ mice were phenotypically normal, as expected from the normal appearance of *cyclin* $D1^{+/-}$ heterozygotes (Fantl et al., 1995; Sicinski et al., 1995).

In order inducibly ablate cyclin D1 expression in adult mice, we crossed *cyclin* $D1^{F/-}$ mice with *Esr1-Cre* animals. The latter strain ubiquitously expresses tamoxifen-inducible Cre recombinase. Administration of tamoxifen to *Esr1-Cre* mice activates Cre, leading to global deletion of the floxed sequences in mouse organs (Hayashi and McMahon, 2002).

Adult *cyclin* $D1^{F/-}$*/Esr1-Cre* mice were injected with tamoxifen, and efficient deletion of cyclin D1 in several organs was verified by semiquantitative PCR (Figure S1D). We then observed the animals for 1 year, without noting any obvious abnormalities or premature lethality. The mice displayed normal biochemical parameters in the peripheral blood, which were periodically monitored (Figures S1E and S1F and data not shown). Hence, acute ablation of cyclin D1 in adult mice had no detectable impact on the animals' health, suggesting that cyclin D1 is largely dispensable for normal physiology of adult animals.

Acute Ablation of Cyclin D1 in Adult Females Bearing *ErbB2*-Driven Mammary Carcinomas

We next asked what would be the consequence of an acute and global ablation of cyclin D1 in mice bearing *ErbB2*-driven mammary carcinomas. We used *MMTV-ErbB2* mice that overexpress *ErbB2* (*HER2*) oncogene in their mammary epithelium (Muller et al., 1988). Female *MMTV-ErbB2* mice develop mammary adenocarcinomas with a median latency of 30–40 weeks (Yu et al., 2001). We interbred *cyclin* $D1^{F/-}$, *Esr1-Cre*, and *MMTV-ErbB2* mice and generated *cyclin* $D1^{F/-}$*/Esr1-Cre/MMTV-ErbB2* females. Once these animals developed palpable breast tumors, we injected them with tamoxifen, thereby triggering cyclin D1 deletion in the whole animal, including in their breast cancers (Figure 1A). We found that ablation of cyclin D1 halted breast cancer progression. For controls, we used *cyclin* $D1^{F/+}$*/Esr1-Cre/MMTV-ErbB2* females, whose tumors continued to grow following tamoxifen challenge (Figure 1B). Consequently, at the time of sacrifice, the animals' overall tumor burden was significantly lower in *cyclin* $D1^{F/-}$*/Esr1-Cre/MMTV-ErbB2* females (Figures 1B, S1G, and S1H).

Staining of tumor sections for Ki-67, a marker of proliferation, revealed a strongly reduced fraction of cells expressing Ki-67 in cyclin D1-deleted tumors, indicating that cyclin D1 shutdown crippled proliferation of breast cancer cells in vivo (Figures S1I and S1J). Strikingly, we observed that cyclin D1 ablation also triggered senescence of breast cancer cells, as evidenced by wide-spread staining of tumor cells for senescence-associated (SA)-β-galactosidase (Figures 1C and 1D) and trimethylated lysine 9 of histone H3 (H3K9-Me3, Figure S1K). These results indicate that the continued presence of cyclin D1 is required to maintain growth of ErbB2-overexpressing breast cancers, by driving tumor cell proliferation and by protecting tumor cells from senescence.

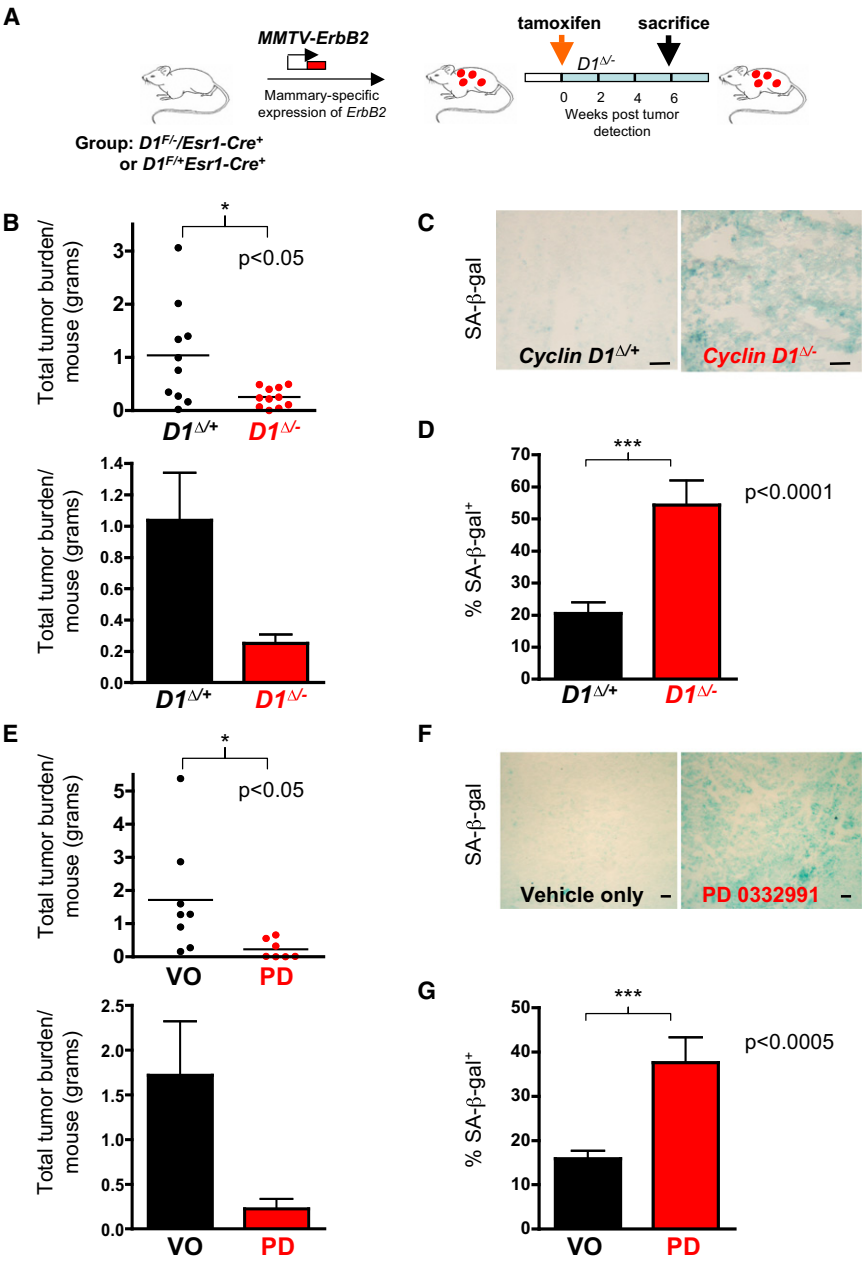

Figure 1. Acute Ablation of Cyclin D1 Blocks Tumor Progression and Triggers Senescence in *ErbB2*-Driven Tumors

(A) Schematic representation of the experimental design.

(B) Total tumor burden per mouse in *cyclin* $D1^{F/+}$/*Esr1-Cre/MMTV-ErbB2* ($D1^{\Delta/+}$) and in $D1^{F/-}$/*Esr1-Cre/MMTV-ErbB2* ($D1^{\Delta/-}$) mice. Deletion of cyclin D1 was induced (by tamoxifen administration) upon detection of palpable tumors; mice were sacrificed after 6 weeks. In the top panel, each dot represents the total tumor burden (g) for a given mouse upon sacrifice, horizontal lines represent mean values. Lower panel: mean total tumor burden (g) per mouse. Error bars represent SD, n = 10.

(C) Representative SA-β-galactosidase staining of sections of *ErbB2*-driven mammary tumors following acute cyclin D1 shutdown (*cyclin* $D1^{\Delta/-}$), or in control animals (*cyclin* $D1^{\Delta/+}$). Scale bar represents 50 μm.

(D) Mean percentage of SA-β-galactosidase-positive area in tumor sections. For each section, three independent areas were scanned and quantified using software from Aperio Technologies. Error bars represent SEM.

(E) Total tumor burden per animal in *MMTV-ErbB2* mice treated daily with vehicle only (VO) or PD 0332991 (PD, 150 mg/kg body weight) for 6 weeks after detection of palpable tumors. Upper panel shows tumor burden for each mouse, lower panel shows mean values ± SD, n = 7.

(F) Representative SA-β-galactosidase staining of sections of *ErbB2*-driven mammary carcinomas from mice treated with vehicle only or PD 0332991 for 6 weeks after detection of palpable tumors. Scale bar represents 50 μm.

(G) Mean percentage of area staining positive for SA-β-galactosidase, analyzed as in (D). Error bars represent SEM.

See also Figure S1.

Inhibition of Cyclin D-Cdk Kinase Activity in Adult Females Bearing *ErbB2*-Driven Mammary Tumors

We next asked whether inhibition of cyclin D-associated kinase activity would have the same impact as an acute cyclin D1 ablation. To address this issue, we monitored a group of *MMTV-ErbB2* females for breast cancer occurrence. As soon as breast tumors were detected, we started treating mice with PD 0332991, a specific and potent inhibitor of cyclin D-CDK4 and D-CDK6 kinases (Fry et al., 2004). We found that inhibition of cyclin D-associated kinase activity essentially phenocopied an acute cyclin D1 ablation, namely it halted progression of breast cancers, and it triggered tumor cell senescence (Figures 1E–1G, S1L, and S1M), without having any overt effect on the animals' health (data not shown). Neither cyclin D1 ablation nor PD 0332991 treatment had any effect on the apoptotic rate of breast cancer cells (Figure S1N).

Collectively, these analyses revealed that cyclin D1 and cyclin D1-associated kinase are largely dispensable for the physiology of adult animals, but they are essential for maintenance of *ErbB2*-driven breast cancers.

Molecular Analyses of *ErbB2*-Driven Breast Cancers

In order to gain some understanding of the observed antisenescence function of cyclin D1-associated kinase in breast cancers in vivo, we first focused on the pRB → E2F pathway. Hypophosphorylated (active) pRB protein was shown to enforce the senescent state by permanently silencing expression of E2F target genes, such as *cyclin E1*, *cyclin A2*, or *Dhfr* (Chicas et al., 2010; Narita et al., 2003; Dean et al., 2010). We found that administration of PD 0332991 to breast cancer-bearing animals resulted in a strong inhibition of pRB phosphorylation in breast cancer cells in vivo (Figure S1O). This led to decreased

expression of E2F target genes, including the genes whose silencing was implicated to play a role in the senescence program (Figure S1P). We conclude that inhibition of E2F activity likely contributes to cancer cell senescence in vivo.

We recently showed that cyclin D1-CDK4 kinase phosphorylates, stabilizes, and activates FOXM1 transcription factor (Anders et al., 2011), which plays an important role in protecting cancer cells from senescence (Li et al., 2008a; Park et al., 2009). Moreover, treatment of in vitro cultured human cancer cells with PD 0332991 destabilized FOXM1 and led to pRB-independent cancer cell senescence (Anders et al., 2011). Analyses of breast tumors from PD 0332991-treated mice revealed significantly decreased levels of FOXM1 protein in cancer cells in vivo (Figure S1Q). We also established that this led to significantly reduced levels of FOXM1 transcriptional targets (Figure S1R). It is likely that this inhibition of FOXM1 activity contributes to senescence of breast cancer cells in vivo, upon PD 0332991-administration to cancer-bearing mice. It should be noted, however, that because we ablated cyclin D1, or inhibited cyclin D1-associate kinase in the entire animal (not only in tumor cells) we cannot exclude that noncell autonomous mechanisms contributed to inhibition of tumor progression.

Ablation of Cyclin D3 in Adult Mice

Another instance of a specific requirement for a particular D-cyclin in tumor initiation is the reliance of T cell acute lymphoblastic leukemia (T-ALL) formation on cyclin D3. We previously showed that *cyclin D3*$^{-/-}$ mice are refractory to *Notch1*-driven T-ALL (Sicinska et al., 2003). To determine whether T-ALL cells also require this cyclin for tumor maintenance, we generated conditional cyclin D3 knockout (*D3*$^{F/F}$) mice (Figures S1S–S1U).

We crossed *cyclin D3*$^{F/F}$ and *Esr1-Cre* mice and obtained cyclin *D3*$^{F/F}$*/Esr1-Cre* animals. We challenged adult *cyclin D3*$^{F/F}$*/Esr1-Cre* mice with tamoxifen, verified efficient deletion of the floxed cyclin D3 alleles in multiple organs (Figure S1V), and observed mice for 1 year. We found no obvious abnormalities upon cyclin D3 ablation throughout the entire observation period, including normal biochemical parameters in the peripheral blood, which were periodically monitored (Figure S1E).

Because *cyclin D3*$^{-/-}$ mice displayed hematopoietic abnormalities (Sicinska et al., 2003, 2006; Cooper et al., 2006), we also crossed *cyclin D3*$^{F/F}$ mice with *Mx1-Cre* animals. The latter strain allows a very efficient inducible deletion of the floxed sequences in the hematopoietic cells, following administration of polyI-polyC (pI-pC) (Kühn et al., 1995) (Figure S2A). We found that an acute shutdown of cyclin D3 in the hematopoietic lineages of *cyclin D3*$^{F/F}$*/Mx1-Cre* animals essentially phenocopied the abnormalities observed in constitutive cyclin D3 null mice. Specifically, *cyclin D3*$^{\Delta/\Delta}$*/Mx1-Cre* animals displayed very small thymi containing significantly reduced numbers of double-positive CD4$^+$CD8$^+$ thymocytes (Figures S2B and S2C). Analyses of peripheral blood revealed modestly decreased red and white blood cell counts (Figures S2D–S2F), again resembling the abnormalities found in *cyclin D3*$^{-/-}$ animals (Sicinska et al., 2006). Altogether, these observations revealed that an acute shutdown of cyclin D3 recapitulated the phenotype of cyclin D3 null mice, but it did not cause any additional major abnormalities, indicating that cyclin D3 is largely dispensable for the health of adult animals.

Ablation of Cyclin D3 in T-ALL

We next asked what would be the impact of an acute shutdown of cyclin D3 for development and maintenance of T cell acute lymphoblastic leukemia. As before, we utilized a mouse model of *Notch1*-driven T-ALL, as the majority of human T-ALL cases contain activating lesions in the Notch1 pathway (Weng et al., 2004). We collected bone marrow cells from *cyclin D3*$^{F/F}$*/Mx1-Cre*$^+$ or *D3*$^{F/F}$*/Mx1-Cre*$^-$ mice, flow-sorted hematopoietic progenitor cells (HPC), transduced HPC with a retrovirus encoding activated *Notch1* (Notch1 intracellular domain, *Notch1-ICD*) and GFP, and injected the transduced HPC into the bloodstream of sublethally irradiated C57BL/6 wild-type recipient mice (Figure 2A). It is well established that the recipient animals develop T-ALL following this procedure. The first abnormal, GFP-positive CD4$^+$CD8$^+$ cells appear in the peripheral blood after ~2 weeks, mice develop multiple T cell tumors after 6 weeks, leading to the animals' death within 10–12 weeks (Li et al., 2008b; Chiang et al., 2006).

Two weeks after bone marrow transplantation (BMT), when abnormal GFP$^+$ cells appeared in the peripheral blood, we challenged the recipient mice with pI-pC to ablate cyclin D3 expression in the transplanted cells. Unexpectedly, we found that the GFP$^+$ cells essentially disappeared from the peripheral blood following cyclin D3 shutdown (Figures 2B and 2C). Further observation of animals revealed that whereas control mice (transduced with *cyclin D3*$^{F/F}$*/Mx1-Cre*-negative HPC) developed T cell tumors and died within 11 weeks, six out of seven mice that sustained acute cyclin D3 deletion remained leukemia-free and healthy throughout the observation period (Figure 2D). We found that in the single experimental mouse that succumbed to T-ALL, tumors arose from the residual cells containing undeleted *cyclin D3* alleles (Figure S3A). The remaining six mice were eventually sacrificed after 30 weeks, and the absence of infiltrating leukemic cells in their organs was verified by detailed histopathological analysis (Figure S3B). Hence, an acute ablation of cyclin D3 blocked development of *Notch1*-driven T-ALL in vivo.

In the analyses described above, we deleted cyclin D3 at an early time-point of T-ALL development. To investigate the requirement for cyclin D3 in the maintenance of T-ALL tumors, we next switched off cyclin D3 expression (by pI-pC administration) at 6.5 weeks post-BMT, after the animals had developed tumors (Figure 3A). We then collected major organs and enumerated the presence of infiltrating GFP$^+$ tumor cells, by FACS. Strikingly, we found that an acute ablation of cyclin D3 led to a strong reduction in the number of tumor cells (Figures 3B and 3C; data not shown). Long-term observation of animals revealed that ablation of cyclin D3 led to a significant extension of the animals' survival (Figure 3D). We verified that tumors which eventually arose in these animals contained GFP$^+$ cells with undeleted *cyclin D3*^{F} alleles (Figure S3C). Collectively, these analyses established that cyclin D3 is required for maintenance of *Notch1*-driven T-ALL in vivo, and that an acute ablation of cyclin D3 leads to disappearance of malignant cells.

Cell Cycle Arrest and Tumor Cell Apoptosis Following Ablation of Cyclin D3

To examine the cellular mechanisms by which cyclin D3 ablation inhibits *Notch1-ICD*-induced T-ALL progression, we first

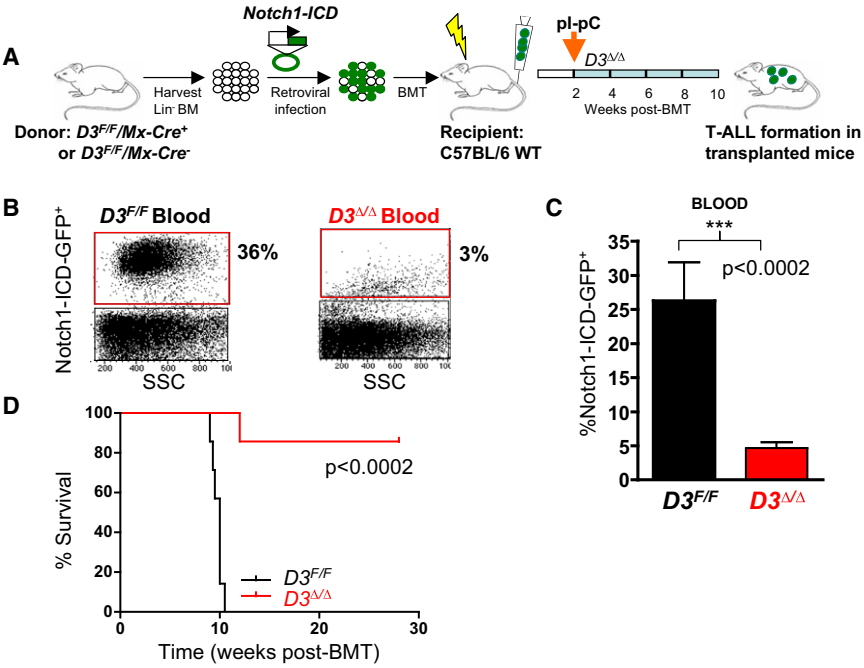

Figure 2. Acute Ablation of Cyclin D3 in a Mouse Model of *Notch1-ICD*-Driven T Cell Acute Lymphoblastic Leukemia

(A) Schematic representation of the experimental design. After T-ALL formation in the recipient mice, cyclin D3 ablation was induced at 2 weeks post-BMT.

(B) Representative FACS profiles showing percentage of *Notch1-ICD*-overexpressing GFP$^+$ cells in peripheral blood right after completion of pI-pC administration (started 2 weeks post-BMT) to *cyclin D3$^{F/F}$/Mx1-Cre$^+$*(*D3$^{\Delta/\Delta}$*) or *D3$^{F/F}$/Mx1-Cre$^-$* (*D3$^{F/F}$*) mice. SSC, side scatter.

(C) Mean percentages of GFP$^+$ cells in peripheral blood of mice treated as in (B). Error bars represent SD, n = 7.

(D) Kaplan-Meier analysis of survival time in each group, n = 7.

See also Figure S2.

examined cell cycle distribution of splenic tumor cells following an acute shutdown of cyclin D3. We observed a reduction of cells in the S phase and an increase of G0/G1 cells (Figures S4A–S4C). We next asked whether the rapid disappearance of T-ALL cells upon cyclin D3 ablation might be caused by tumor cell apoptosis. To test this, we stained the GFP$^+$ leukemic cells from the peripheral blood, as well as tumor cells that infiltrated spleens, with Annexin V/7-AAD, and analyzed by FACS. We detected wide-spread apoptosis of peripheral blood leukemic cells and of tumor cells following cyclin D3 ablation (Figures 4A–4D). TUNEL staining of tumor sections confirmed tumor cell apoptosis (Figure 4E). These analyses revealed that cyclin D3 is required to maintain survival of T-ALL cells, and that ablation of cyclin D3 triggers tumor cell apoptosis.

Tumor Cell Apoptosis following Inhibition of Cyclin D-Cdk Kinase

We wished to determine whether inhibition of cyclin D3-associated kinase activity would have the same impact as an acute cyclin D3 ablation. To address this, mice were injected with wild-type hematopoietic progenitor cells that were transduced with a virus expressing Notch1-ICD and GFP, leading to T-ALL development. Daily treatment with PD 0332991 was started when GFP$^+$ cells were detected in the peripheral blood (2 weeks posttransplantation), or after mice had developed T cell tumors (6.5 weeks posttransplantation). Once the treatment was initiated, we observed a strong reduction in the number of leukemic cells in the peripheral blood and of tumor cells infiltrating the peripheral organs (Figures 5A and 5B; data not shown). Continuous long-term treatment resulted in a dramatic improvement of survival rates in both groups, with the majority of animals remaining healthy at 40 weeks post-BMT (Figures 5C and 5D). Importantly, we verified that treatment of tumor cells with PD 0332991 inhibited cell cycle progression and triggered tumor cell apoptosis, thereby mimicking the effect of an acute cyclin D3 ablation (Figures 5E, 5F, S5A, and S5B data not shown). Moreover, combined administration of pI-pC (to induce deletion of cyclin D3) plus PD 0332991 to *cyclin D3$^{F/F}$/Mx1-Cre* mice did not increase the tumor apoptotic rate above that seen upon cyclin D3 ablation alone, confirming that the effects of PD 0332991 are mediated by inhibiting cyclin D3 activity (Figure S5C). No senescence of T-ALL cells was observed following PD 0332991 treatment (Figure S5D). Collectively, these findings indicate that cyclin D3-Cdk kinase is required for T-ALL maintenance, by driving cell proliferation and by protecting tumor cells from the apoptotic death.

Analyses of Human Leukemic Cells In Vitro and In Vivo

We next asked whether inhibition of cyclin D-associated kinase activity in human leukemic cells would also trigger apoptosis. We chose human T-ALL cell lines KOPTK1, DND41, MOLT-16, and RPMI-8402, which are known to harbor activating mutations in the *NOTCH1* gene (*NOTCH1-ICD*-positive) (O'Neil et al., 2007). We treated cells in vitro with PD 0332991, stained them with Annexin V/7-AAD, and analyzed by FACS. We observed that inhibition of cyclin D-CDK kinase triggered cell cycle arrest and apoptosis of human T-ALL cells (Figures 6A, 6B, S6A, and S6B; data not shown). No senescence of T-ALL cells was observed after PD 0332991 treatment (Figure S6C).

Similar analysis of an additional 20 human leukemic cell lines (including *NOTCH1-ICD*-negative T-ALL, B cell ALL, and others) revealed that PD 0332991 treatment did not cause substantial increase in the apoptotic rate in these cell lines (Figure S6D; data not shown). This, together with our observations that inhibition of cyclin D3 activity killed *Notch1-ICD*-positive mouse T-ALL tumor cells (Figures 4 and 5), suggests that cyclin D3-CDK activity is specifically required for survival of T-ALL cells with activated Notch1 pathway.

Intriguingly, comparison of the levels of D-cyclins and CDKs between four *NOTCH1-ICD*-positive and negative human

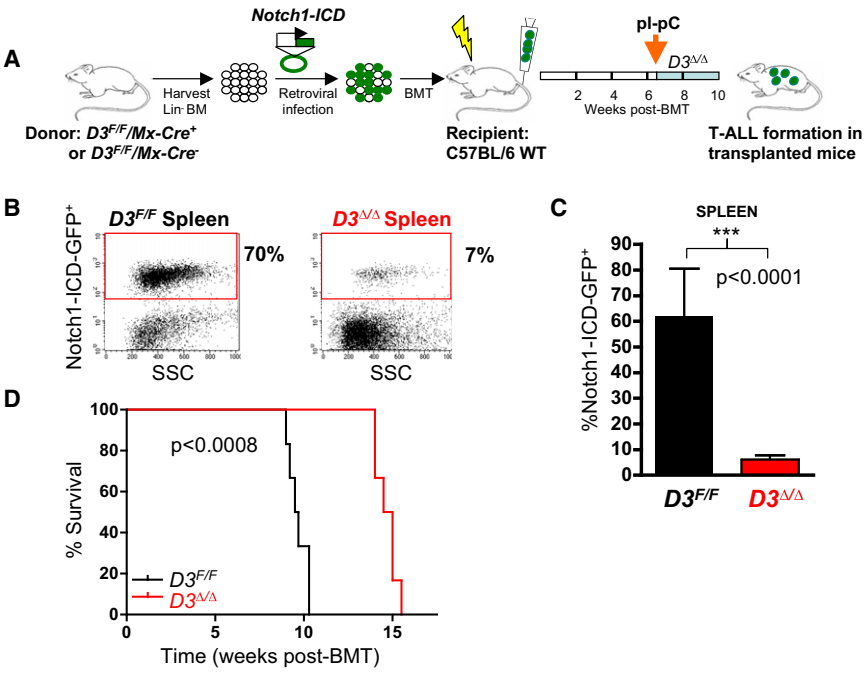

Figure 3. Cyclin D3 Is Required for Maintenance of *Notch1-ICD*-Driven T-ALL In Vivo

(A) Schematic representation of the experimental design. After T-ALL formation in the recipient mice, cyclin D3 ablation was induced at 6.5 weeks post-BMT.

(B) Representative FACS analysis showing percentage of Notch1-ICD-overexpressing GFP^+ cells in spleens right after completion of pI-pC administration (started 6.5 weeks post-BMT) in *cyclin* $D3^{F/F}$/*Mx1-Cre*$^+$ ($D3^{\Delta/\Delta}$) or $D3^{F/F}$/*Mx1-Cre*$^-$ ($D3^{F/F}$) mice. SSC, side scatter.

(C) Mean percentages of GFP^+ cells in spleens of mice treated as in (B). Error bars represent SD, n = 4.

(D) Kaplan-Meier analysis of survival time in each group, n = 6.

See also Figure S3.

T-ALL lines indicated that the former express significantly higher levels of cyclin D3 (and cyclin D2) and cyclin D3-CDK6 complexes (Figures S6E and S6F). It is possible that NOTCH1 activation increases the levels of D-cyclins in T-ALL cells, thereby making these cells "addicted" to cyclin D-CDK kinase for tumor cell survival.

To test the response of human *NOTCH1-ICD*-positive T-ALL cells to cyclin D-CDK inhibition in an in vivo setting, we engineered the human T-ALL cell lines KOPTK1 and DND41 to stably express firefly luciferase. Engineered human leukemic cells were injected intravenously into immunocompromised mice, and bioluminescence imaging was used to assess the distribution and burden of leukemic disease. Recipient mice died within 5–7 weeks due to widely disseminated T cell leukemia.

To determine the acute effects of CDK4/6 inhibition, mice with disseminated KOPTK1 and DND41 leukemia were treated for 5–7 days with PD 0332991. As expected, leukemic burden increased in vehicle-treated mice (Figures 7A and 7C). In contrast, treatment with PD 0332991 either resulted in a nearly 5-fold reduction in tumor burden (KOPTK1 cells, Figure 7A) or blunted this increase (DND41, Figure 7C). We collected peripheral blood and bone marrow cells from PD 0332991 treated animals, and analyzed the proportion of apoptotic human T-ALL cells by Annexin V/7-AAD staining followed by FACS. Treatment of tumor-bearing mice with PD 0332991 induced significant apoptosis in both KOPTK1 (Figure 7B) and DND41 (Figure 7D) xenografts in vivo without having any overt effect on the animals' health (Figure S7; data not shown).

To determine the therapeutic efficacy of CDK4/6 inhibition, we treated mice bearing established human T-ALL xenografts with PD 0332991. Long-term daily treatment with PD 0332991 resulted in suppression of leukemia progression as determined by bioluminescence imaging (Figures 7E, 7F, 7H, and 7I), and resulted in a highly significant prolongation in survival for both KOPTK1 (Figure 7G) and DND41 (Figure 7J) xenografted animals. Collectively, these findings suggest that inhibition of cyclin D-associated kinase activity in patients with *NOTCH1*-positive T-ALL might represent an attractive therapeutic approach, as it may lead to selective killing of leukemic cells.

Molecular Analyses of T-ALL Cells and Breast Cancer Cells

The studies described above revealed that T-ALL cells respond to inhibition of cyclin D-CDK4/6 kinase by undergoing cell cycle arrest and cell death. In order to understand the molecular basis of these phenomena, we first focused on the pRB → E2F pathway. We observed that treatment of T-ALL cells with PD 0332991 resulted in the appearance of hypophosphorylated (active) pRB species (Figures S5A, S5B, S6A, and S6B). Inhibition of cyclin D3 function led to diminished E2F transcriptional activity, as evidenced by decreased levels of several E2F transcriptional targets, including genes involved in G1 and S phase progression (Figure S4C). We conclude that inhibition of the pRB → E2F pathway is likely responsible for cell cycle arrest of T-ALL cells following PD 0332991 treatment.

The pRB → E2F pathway was shown to be also involved in controlling cell survival (Ianari et al., 2009; Young and Longmore, 2004). E2Fs can play both pro-survival and pro-apoptotic roles, depending on cellular context (Chen et al., 2009; Chong et al., 2009). In the developing mouse retinas, E2Fs were shown to play a pro-survival function by inducing expression of p53-deacetylating enzymes. Ablation of E2Fs in retinal cells was demonstrated to cause strong hyperacetylation of p53, leading to p53 activation and p53-dependent cell death (Chen et al., 2009). However, we found that cyclin D3-CDK kinase likely does not operate through this mechanism in T-ALL cells. First, we established that PD 0332991 treatment did not overtly change p53 acetylation levels in T-ALL cells (Figure S5E). Moreover, cyclin D-CDK4/6 inhibition also triggered apoptosis of T-ALL cell lines expressing mutant p53: MOLT-16, DND-41, and RPMI-8402 (http://www.sanger.ac.uk/genetics/CGP/CellLines/)

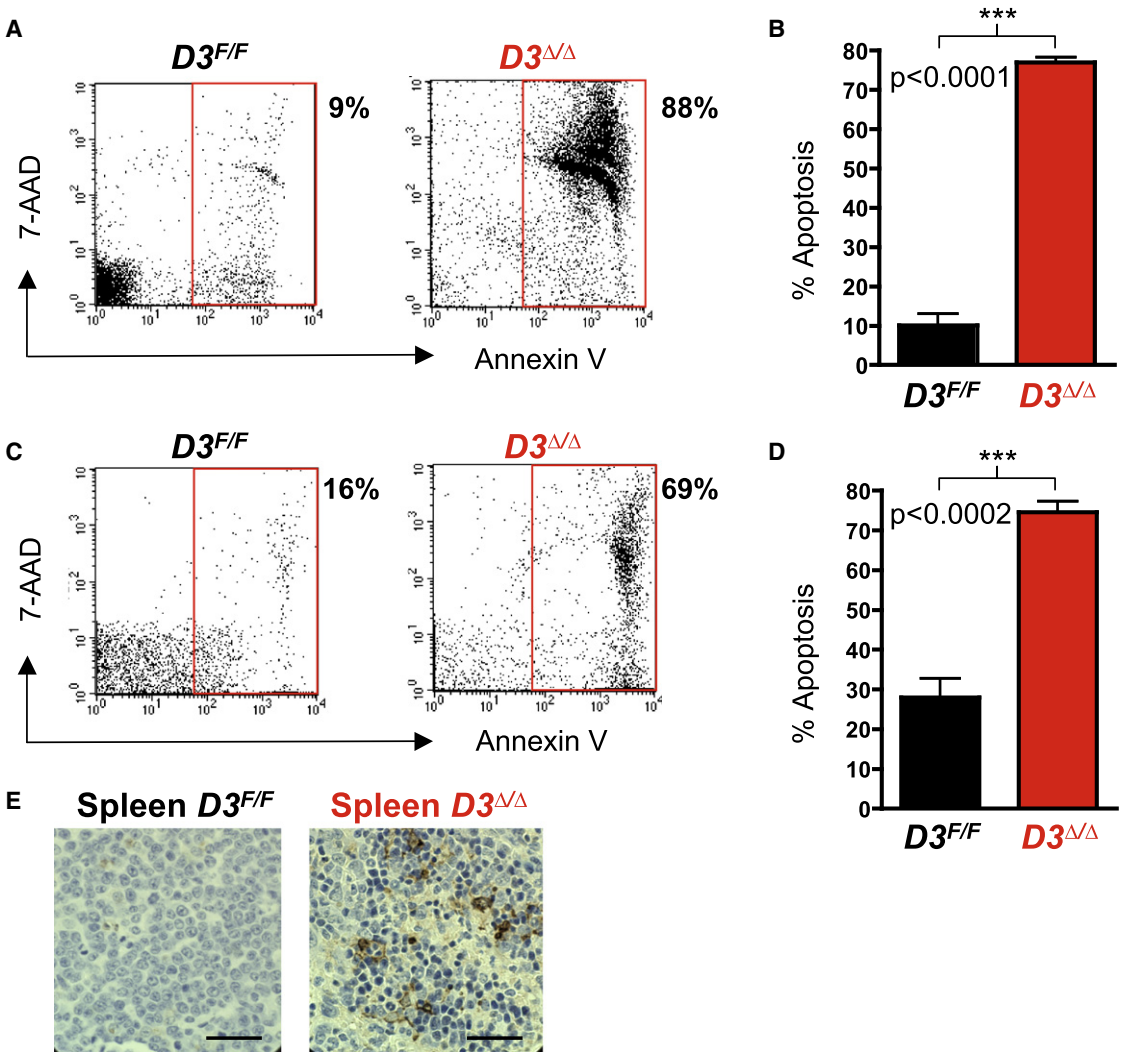

Figure 4. Cyclin D3 Ablation Triggers Apoptosis of *Notch1-ICD*-Driven T-ALL Cells

Mice received *Notch1-ICD*-GFP-transduced *cyclin D3$^{F/F}$/Mx1-Cre^{+}* (*D3$^{Δ/Δ}$*) or *D3$^{F/F}$/Mx1-Cre^{-}* (*D3$^{F/F}$*) bone marrow cells, and were treated five times with pI-pC, starting at 6.5 weeks following BMT.

(A) Representative FACS profiles of peripheral blood stained for Annexin V/7-AAD and gated on GFP^{+} cells.

(B) Mean percentages of apoptotic (Annexin V^{+}) cells in peripheral blood (gated on GFP^{+} cells) and analyzed as in (A). Error bars represent SD, n = 4.

(C) Representative FACS profiles of cells from the spleen stained for Annexin V/7-AAD and gated on GFP^{+}.

(D) Mean percentages of apoptotic (Annexin V^{+}) cells from spleens (gated on GFP^{+} cells) and analyzed as in (C). Error bars represent SD, n = 4.

(E) TUNEL staining of spleen sections. Scale bar represents 50 μm.

See also Figure S4.

(Figure 6), indicating that the apoptosis following cyclin D-CDK4/6 inhibition can be p53-independent.

Given a differential response to PD 0332991 treatment of T-ALL cells (cell cycle arrest and apoptosis) versus breast cancer cells (cell cycle arrest and senescence, but no apoptosis), we decided to compare the response of these two tumor types to cyclin D-CDK4/6 inhibition at a molecular level. To this end, we treated in vitro cultured human T-ALL cell line KOPTK1 and mouse breast cancer cells derived from *MMTV-ErbB2* tumor (V720 cells) (Yu et al., 2006) with PD 0332991. We then analyzed gene expression at a genome-wide level using microarrays.

Comparison of T-ALL and breast cancer cell expression profiles revealed three distinct gene expression groups (Figure 8A; Tables S1–S4). The first group comprised of genes that change their expression upon PD 0332991 treatment both in T-ALL and in breast cancer cells. We observed a strong enrichment for "cell cycle" genes by gene ontology analysis in this group (Table S2). Analysis of all cell cycle genes that were significantly regulated by PD 0332991 treatment indicated that the majority of them were downregulated (Figure 8B), which likely explains the observed cell cycle arrest.

The second group comprised of genes that, upon PD 0332991 treatment, change their expression in T-ALL, but not in breast cancer cells (Figure 8A). This group showed strong enrichment for "apoptosis" genes by gene ontology analysis (Table S3). Analysis of all apoptosis-related genes that were significantly

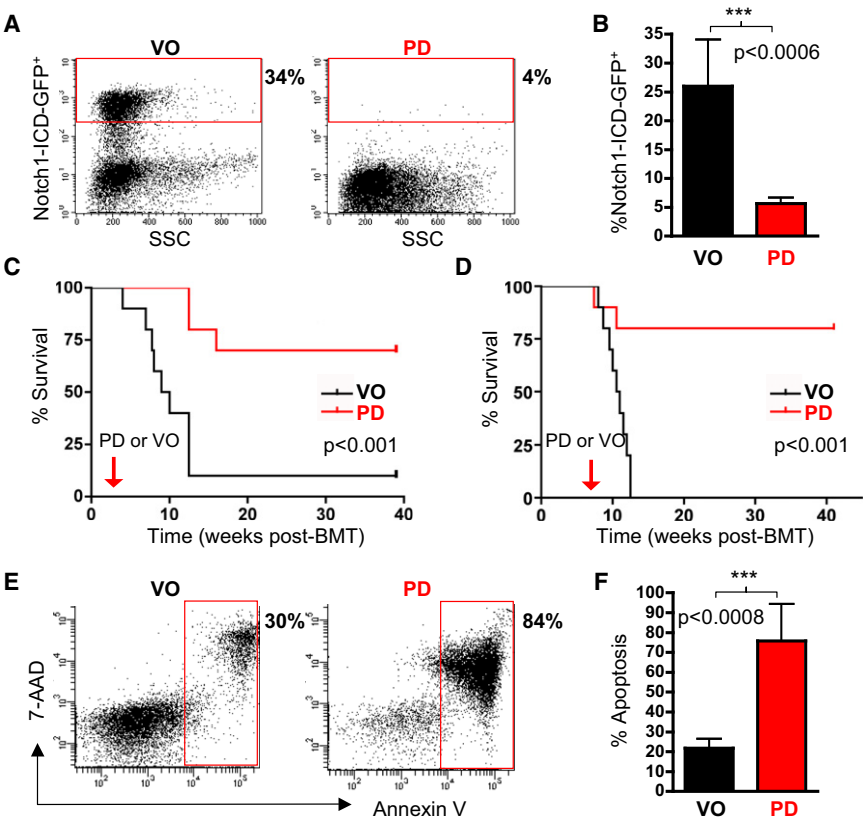

Figure 5. Pharmacological Inhibition of Cdk4/6 Activity in *Notch1-ICD*-Driven T-ALL

Mice received *Notch1-ICD*-GFP-transduced C57BL/6 wild-type bone marrow cells, and were fed daily with either vehicle only (VO) or Cdk4/6 inhibitor, PD 0332991 (PD, 100–150 mg/kg body weight).

(A) PD 0332991 treatment was started at 6.5 weeks post-BMT. Shown are representative FACS profiles depicting percentage of GFP$^+$ cells in peripheral blood after 7 days of PD 0332991 administration. SSC, side scatter.

(B) Mean percentages of GFP$^+$ cells in peripheral blood, in mice treated as in (A). Error bars represent SD, n = 7.

(C and D) Kaplan-Meyer survival curves. (C) Treatment was started at 2 weeks post-BMT (following detection of GFP$^+$ cells in peripheral blood), n = 10 mice per group. (D) Treatment started at 6.5 weeks post-BMT, after animals had developed tumors, n = 10 mice per group.

(E and F) Splenocytes from vehicle treated moribund mice were cultured in vitro and treated with vehicle only (VO) or 1 μM of PD 0332991 (PD) for 4 days. Cells were then stained for Annexin V/7-AAD, and analyzed by FACS.

(E) Shown is a representative FACS profile of Annexin V/7-AAD staining gated on GFP$^+$ splenic tumor cells.

(F) Mean percentage of apoptotic (Annexin V$^+$) tumor cells following treatment with vehicle only or 1 μM of PD. Error bars represent SD, n = 4.

See also Figure S5.

regulated in KOPTK1 cells by PD 0332991 treatment revealed that those genes displayed both up- or downregulation after treatment (Figure 8C). Visual inspection of these genes revealed that cyclin D-CDK4/6 inhibition led to a strong downregulation of *BIRC5*/*Survivin*, and resulted in an upregulation of components of the extrinsic apoptotic pathway (*TNF*, *CASP8*, *CASP10*), upregulation of pro-apoptotic *BIM*, as well an upregulation of *GZMA* and *GZMB* (Figure 8D).

The third group (Figure 8A) contained genes, which change their expression in breast cancer cells, but not in T-ALL cells. This group showed enrichment for "cell division" genes as well for "TGF-β," consistent with the well-established role of TGF-β in cellular senescence (Kuilman and Peeper, 2009) (Table S4).

Collectively these analyses suggest that inhibition of cyclin D-CDK4/6 kinase in *NOTCH1*-positive T-ALL cells triggers a transcriptional apoptotic program, thereby causing death of tumor cells.

DISCUSSION

The causative role of cyclin D overexpression in the pathogenesis of human cancers has been very well documented. Amplification and rearrangements of the *cyclin D1* gene were observed in nearly 100% of mantle cell lymphomas, a substantial fraction of multiple myelomas, and in several other cancer types including breast, squamous cell, pancreatic, endometrial, and lung carcinomas. Also genes encoding cyclin D2 or D3 are frequently amplified in human lymphoid malignancies and in testicular cancers (Deshpande et al., 2005; Fu et al., 2004; Musgrove et al., 2011). Overexpression of cyclin D proteins, which results from these genomic abnormalities, is believed to represent an early, causative event in tumor formation (Chaganti and Houldsworth, 2000; Deshpande et al., 2005; Musgrove et al., 2011). For example, in breast cancers, cyclin D1 overexpression represents one of the earliest oncogenic lesions, seen already in ductal carcinoma in situ (Weinstat-Saslow et al., 1995). Consistent with the role of overexpressed D-cyclins as drivers of the oncogenic process, transgenic mice engineered to overexpress cyclin D1 in mammary glands are prone to mammary carcinomas (Wang et al., 1994). Also, targeted overexpression of cyclin D1 in B lymphocytes was shown to cooperate with the Myc oncogene in triggering B cell lymphomas (Bodrug et al., 1994; Lovec et al., 1994).

Analyses of knockout mice lacking individual D-cyclins supported an essential role for these proteins in tumor initiation. Thus, mice lacking cyclin D1, or its catalytic partner, Cdk4, are either resistant, or show significantly reduced sensitivity to *Ras*- and *ErbB2*-driven breast tumors, depending on the genetic background and type of transgene used (Bowe et al., 2002; Reddy et al., 2005; Yu et al., 2001, 2006; Zhang et al., 2011). Loss of cyclin D1 also renders mice resistant to rhabdoid tumors arising in *Ini1* heterozygotes, decreases intestinal tumorigenesis in Apc^{Min} background, and reduces incidence of *Ras*-driven skin papillomas (Hulit et al., 2004; Robles et al., 1998; Tsikitis et al., 2005). Cyclin D2 null mice show decreased incidence of ovarian and testicular tumors (Burns et al., 2003), whereas mice lacking cyclin D3 or Cdk6, are resistant to *Notch1*-driven T cell acute

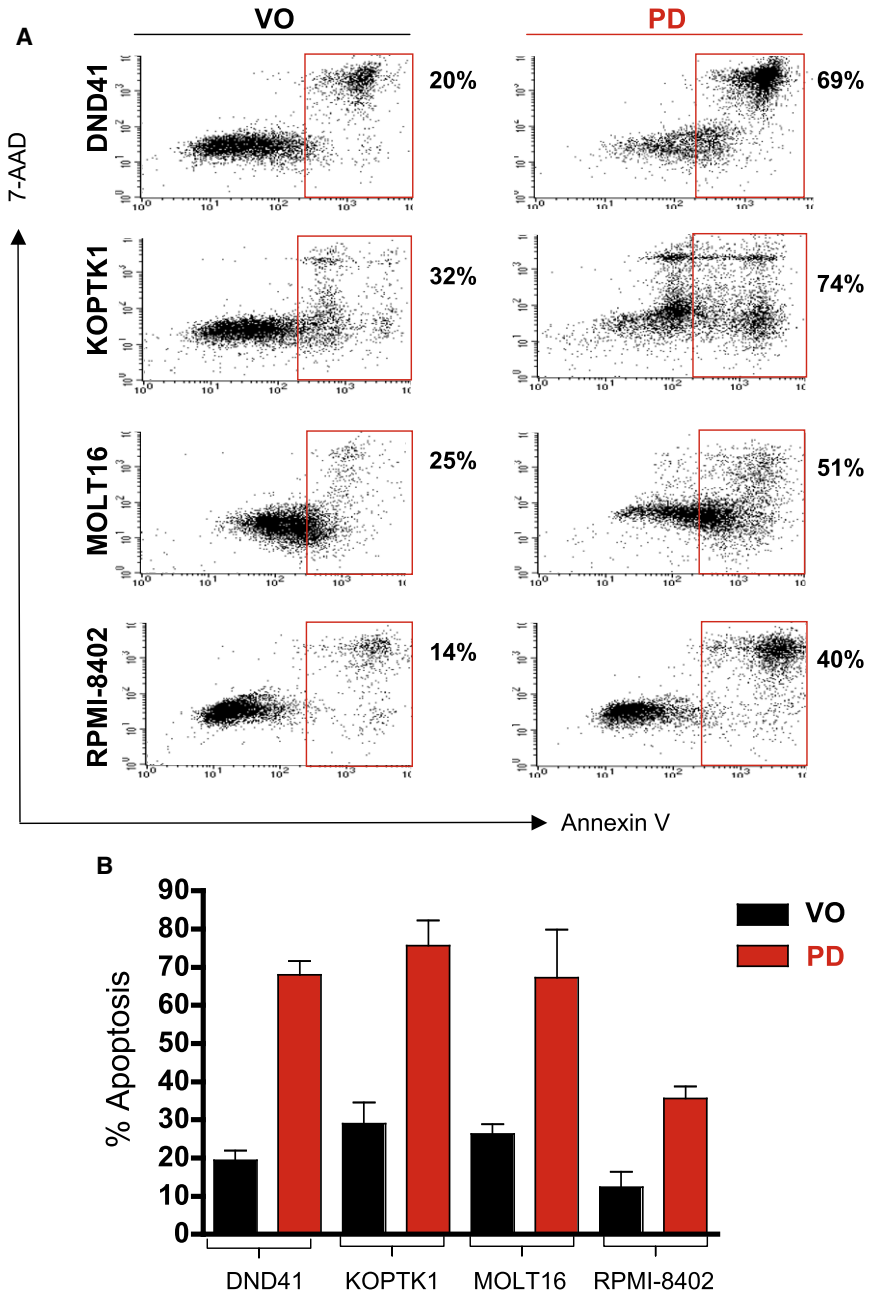

Figure 6. Pharmacological Inhibition of CDK4/6 Kinase Triggers Apoptosis of Human T-ALL Cell Lines

Human T-ALL cell lines were cultured and treated with vehicle only (VO) or 1 μM of PD 0332991 (PD) for 4 days, stained for Annexin V/7-AAD and analyzed by FACS.

(A) Shown are representative FACS profiles of KOPTK1, DND41, MOLT-16, and RPMI-8402 cells stained with Annexin V/7-AAD.

(B) Quantification of the apoptotic (Annexin V^+) cells, analyzed as above. Shown are mean values. Error bars represent SD, n = 4.

See also Figure S6.

lymphoblastic leukemias, or to lymphomagenesis triggered by activated *Akt* (Hu et al., 2009; Sicinska et al., 2003).

All these observations point to the requirement for a D-cyclin in oncogenic transformation. However, in order to validate therapeutic targeting of D-cyclins in cancer treatment one must establish whether the continued presence of these proteins is required to maintain tumor progression. Another critically important question is what would be the consequence of an acute and global ablation of a D-type cyclin in a living animal. To address these issues, we developed mouse strains that allowed us to globally shut down expression of individual D-cyclins in mice that developed different types of tumors. We report here that an acute ablation of cyclin D1 in adult mice bearing *ErbB2*-driven breast cancers halted tumor progression, and triggered senescence of cancer cells, without compromising the animals' health. We also found that an acute ablation of cyclin D3 blocked T-ALL progression by triggering tumor cell apoptosis. Similar effects were seen upon inhibition of cyclin D-Cdk kinase in vivo, by PD 0332991 administration to tumor-bearing animals. Collectively, these results reveal that individual D-cyclins are not required for normal mouse physiology, but they are absolutely essential for tumor maintenance. Hence, by targeting particular D-cyclins, or by inhibiting their associated kinases, one can selectively kill tumor cells, or irreversibly arrest their proliferation by triggering tumor cell senescence, without affecting normal tissues. It remains to be seen whether ablating all three D-cyclins would have any consequences in normal adult animals.

Our results are consistent with recent findings of Puyol et al. (2010) demonstrating that an acute shutdown of Cdk4 in a mouse model of *K-Ras*-driven non-small cell lung cancers triggered senescence of tumor cells in vivo. Together with our results, these findings indicate that cyclin D1-CDK4 antisenescence function likely operates in several cancer types. On the other hand, Zhang et al. (2011) recently reported that *MMTV-ErbB2* breast tumor cells, after two rounds of in vitro and in vivo passaging, no longer require cyclin D1 for proliferation, due to upregulation of cyclin D3. These results indicate that analyses of serially passaged cell lines need to be treated with caution, and should be verified in vivo using intact tumors, as in the work of Puyol et al. (2010) and in this study.

It remains to be determined what makes cancer cells so distinctly dependent on individual D-cyclins. One possibility is that the molecular mechanism of cell cycle progression operates differently in cancer cells versus in normal cells. Moreover, cyclin D-CDK4/6 complexes may play additional, cell

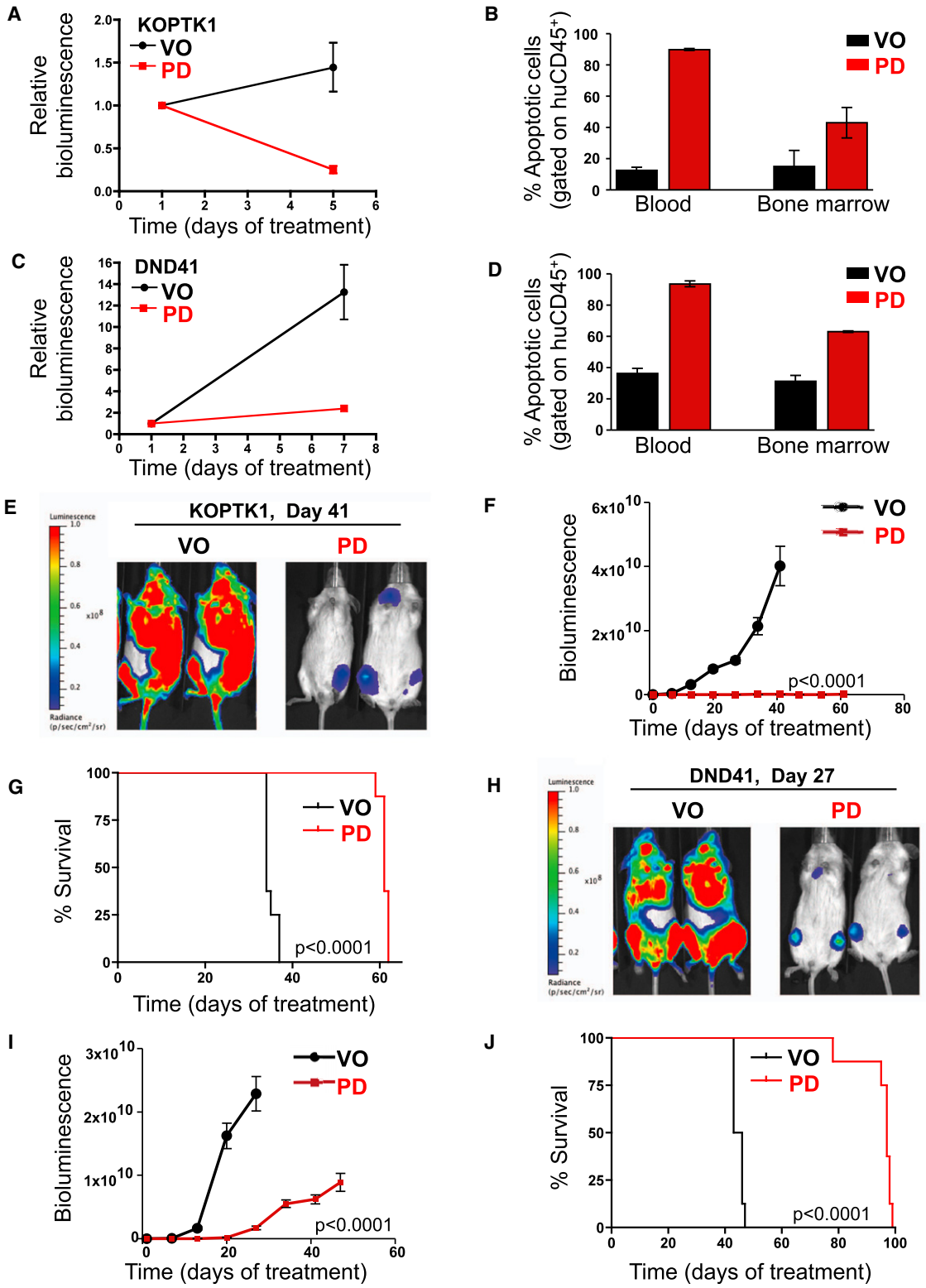

Figure 7. Effects of Pharmacological Inhibition of CDK4/6 on Human T-ALL In Vivo

Human KOPTK1-Luc$^+$ or DND41-Luc$^+$ cells were engrafted by tail vein injection into NSG mice and treated daily with vehicle only (VO) or PD 0332991 (PD, 150 mg/kg body weight).

(A) Animals with established KOPTK1-Luc$^+$ leukemia were treated daily, for 5 days, with vehicle or PD 0332991. Tumor burden is expressed as relative bioluminescence, normalized to the baseline bioluminescence on treatment day 1. Shown are mean values, error bars represent SEM.

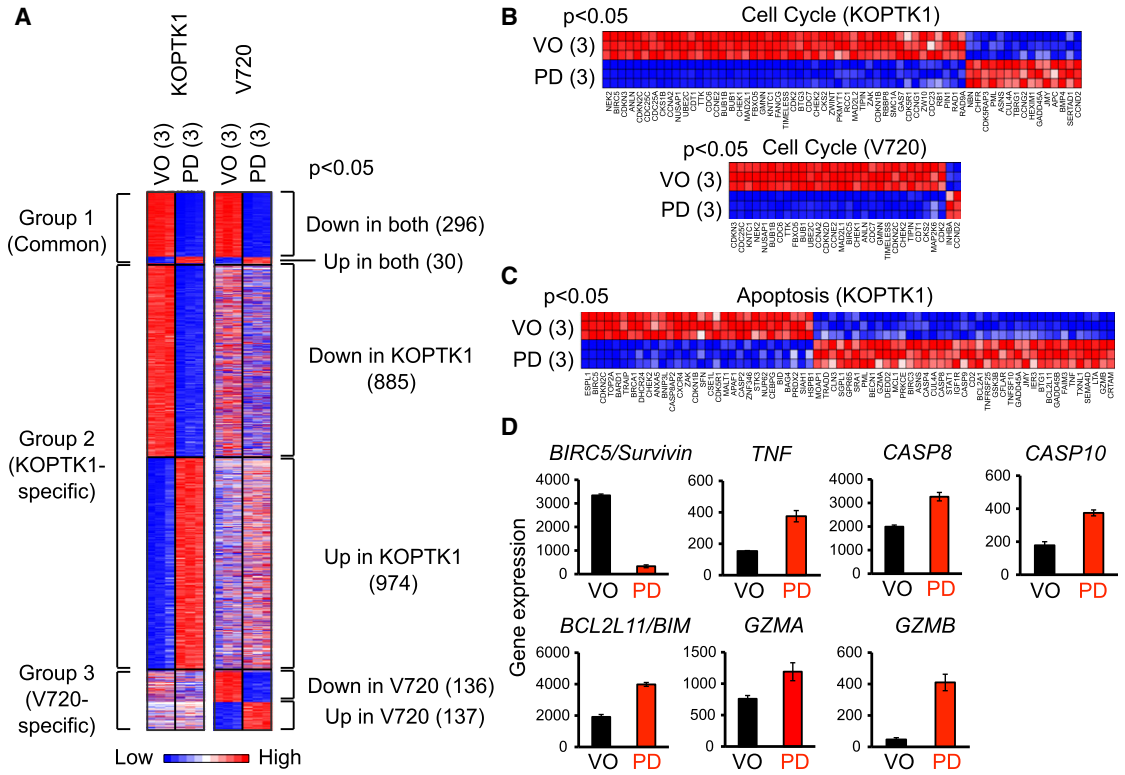

Figure 8. Response of KOPTK1 T-ALL Cells and V720 Breast Cancer Cells to Inhibition of Cyclin D-CDK Kinase

(A) KOPTK1 and V720 cells were treated with PD 0332991 (PD) or vehicle (VO) for 48 hr and 24 hr, respectively. Experiment was done in triplicate. Genes that show changes in expression levels after PD treatment were selected based on an absolute fold-change >1.5, absolute mean difference >50, and p value <0.05, and were classified into three groups: genes with altered expression levels in both cell types (Group 1), in KOPTK1 cells only (Group 2), or in V720 cells only (Group 3). Each row corresponds to one gene and is normalized across the row.

(B) Heatmap images representing relative expression levels of cell cycle-related genes that showed significant expression change after PD treatment in KOPTK1 cells (top) or V720 cells (bottom).

(C) A heatmap image representing relative expression levels of apoptosis-related genes that showed significant expression change after PD treatment in KOPTK1 cells.

(D) Expression levels of seven apoptosis-related genes in KOPTK1 cells. Shown are mean values ± SD, n = 3 per group.

See also Tables S1–S4.

cycle-independent functions in cancer cells, by protecting these cells from oncogene-induced senescence, or by maintaining tumor cell survival. Indeed, cyclin D-CDK kinase was shown to protect cells against senescence, by acting through the retinoblastoma protein (Chicas et al., 2010; Dean et al., 2010; Ruas et al., 2007) and through FOXM1 (Anders et al., 2011). It is likely

(B) After 5 days of treatment, peripheral blood and bone marrow were collected from KOPTK1-Luc$^+$ xenografted animals, and apoptosis of human leukemic cells determined by FACS analysis of Annexin V/7-AAD staining, gated on human CD45$^+$ cells. Graphs represent mean percentages of apoptotic (Annexin V$^+$) cells. Error bars represent SD.

(C) Animals with established DND41-Luc$^+$ leukemia were treated daily, for 7 days, with vehicle or PD 0332991. Tumor burden is expressed as relative bioluminescence, normalized to the baseline bioluminescence on treatment day 1. Shown are mean values, error bars represent SEM.

(D) After 7 days of treatment, peripheral blood and bone marrow were collected from DND41-Luc$^+$ xenografted animals, and apoptosis of human leukemic cells determined by FACS analysis of Annexin V/7-AAD staining, gated on human CD45$^+$ cells. Graphs represent mean percentages of apoptotic (Annexin V$^+$) cells. Error bars represent SD.

(E) Bioluminescence imaging of representative vehicle and PD 0332991 treated KOPTK1-Luc$^+$ xenografted animals.

(F) Total body bioluminescence (photons s^{-1} ROI^{-1}) in vehicle and PD 0332991 treated recipients of KOPTK1-Luc$^+$ cells was monitored over time to determine tumor burden. Shown are mean values, error bars represent SEM.

(G) Kaplan-Meier survival curves of KOPTK1-Luc$^+$ recipients treated with vehicle or PD 0332991.

(H) Bioluminescence imaging of representative vehicle and PD 0332991 treated DND41-Luc$^+$ xenografted animals.

(I) Total body bioluminescence (photons s^{-1} ROI^{-1}) in vehicle and PD 0332991 treated recipients of DND41-Luc$^+$ cells was monitored over time to determine tumor burden. Shown are mean values, error bars represent SEM.

(J) Kaplan-Meier survival curves of DND41-Luc$^+$ recipients treated with vehicle only or PD 0332991. n = 8 for all groups.

See also Figure S7.

that these functions are essential only in certain tumor types, but not in normal tissues, which renders these tumors uniquely sensitive to cyclin D-CDK inhibition.

In contrast to the impact of cyclin D1 inhibition in breast tumors, where it caused tumor cell senescence, we found that the shutdown of cyclin D3 in lymphoid tumors triggered apoptosis. Importantly, we found that cyclin D3-CDK inhibition also resulted in killing of human T-ALL cells in vitro and in vivo. Intriguingly, this effect seems to be specific to *NOTCH1-ICD*-positive T-ALL, suggesting a "synthetic lethal" interaction between activation of the Notch1 pathway and cyclin D-CDK kinase inhibition in leukemic cells. Although the exact molecular mechanism of the observed cell death remains to be determined, our analyses suggest that inhibition of cyclin D-CDK4/6 kinase activity in *NOTCH1-ICD*-positive T-ALL cells triggers a transcriptional apoptotic program, which likely contributes to killing of tumor cells.

Altogether, our study demonstrates that in addition to the well-established roles of overexpressed D-cyclins in tumor initiation, the presence of D-cyclins is essential for tumor maintenance. Our results show that inhibition of cyclin D-kinase activity represents a highly selective anticancer strategy that specifically targets cancer cells without significantly affecting normal tissues.

EXPERIMENTAL PROCEDURES

Full experimental procedures and any associated references are available in the Supplemental Experimental Procedures.

Generation of Conditional *Cyclin D1$^{F/F}$* and *D3$^{F/F}$* Mice

Please see Supplemental Experimental Procedures for details. All animal procedures conformed to the relevant regulatory standards, guidelines, and regulations, and were approved by the Dana Farber Cancer Institute Animal Care and Users Committee. Genotyping and deletion analysis of floxed or deleted *cyclin D1* and *D3* alleles were performed with primers: D1-5′ (5′-GAGTTTTCCGGGTGCGTT-3′), D1-3′ (5′-CTGTGGTGTCGCTGACA-3′), D1-Δ (5′-GGCAGTAGCAAGATCTGTTA-3′) and D3-5′ (5′-CTGCGTTCTGTCCCTTTCCTT-3′), D3-3′ (5′-CGCGATAGACACAGGAACCA-3′), and D3-Δ (5′-CCAGACTGGAGCCAGAGATAA-3′) by predenaturation of genomic DNA at 94°C for 5 min, followed by 33 cycles of amplification: 94°C for 30 s, 60°C for 30 s, 72°C for 30 s, and a final extension step at 72°C for 10 min. The sizes of PCR products are: for *cyclin D1^{wt}* = 180 base pairs (bp), *D1^{F}* = 420 bp, *D1^{Δ}* = 476 bp, *D3^{wt}* = 210 bp, *D3^{F}* = 500 bp, and *D3^{Δ}* = 450 bp. *Cyclin D1$^{F/F}$* mice were bred with *cyclin D1$^{-/-}$* (Sicinski et al., 1995), *Esr1-Cre*, and *MMTV-ErbB2* animals. *Cyclin D3$^{F/F}$* mice were bred with *Esr1-Cre* and *Mx1-Cre* animals. *Mx1-Cre*, *MMTV-ErbB2*, and *Esr1-Cre* mice were from Jackson Laboratory.

Acute Ablation of Cyclins D1 or D3 and PD 0332991 Treatment

Esr1-Cre expressing mice were injected intraperitoneally with 4-hydroxytamoxifen (Sigma) 0.225 mg/g of body weight on alternate days. To inhibit cyclin D-Cdk kinase, mice were fed daily with PD 0332991, 150 mg/kg of body weight by gastric gavage; every 2 weeks the daily dose was lowered to 100 mg/kg for 2–3 days. Control mice were treated with vehicle (10% 0.1N HCl, 10% Cremaphor EL, 20% PEG300, 60% 50 mM citrate buffer pH 4.5) 10 ml/kg by gastric gavage. *Mx1-Cre* expressing mice were injected intraperitoneally with 2.5 μg/g body weight of polyinosinic-polycytidylic acid on alternate days (pI-pC, Amersham).

Flow Cytometry Analysis and Sorting

Cells were stained with antibodies against CD4 and CD8 (BD Biosciences). For cell cycle analyses, mice were intraperitoneally injected with 1–2 mg BrdU and sacrificed after 2hr. Tissues were harvested and analyzed with BrdU-Flow kit using either anti-BrdU antibody conjugated to phycoerythrin (PE) or fluorescein isothiocyanate (FITC) (BD Biosciences). Annexin V/7-AAD staining was performed on fresh cells according to the manufacturer's specifications (ApoScreen, Southern Biotech). Cells from human T-ALL xenotransplants were stained with anti-human CD45 antibody (Biolegend). Alternatively cells were fixed, permeabilized, and stained with phycoerythrin (PE)-mouse anti-phospho pRb^{S780} antibody (BD Biosciences) or isotype IgG1 control and analyzed by FACS. All data acquisition was performed on LSRII, Fortessa and Facscan and analyzed using Cell Quest and FACSDiva software (BD Biosciences). Sorting was conducted on Moflow or FACSaria sorters (BD Biosciences).

In Vitro Analyses of Leukemic Cells

Spleens were collected from moribund vehicle-treated recipients of *Notch1-ICD*- and GFP-expressing tumor cells and cultured for 4 days in RPMI supplemented with 10% fetal calf serum (Sigma) and 10 mM glutamine in the presence of 1μM PD 0332991 or vehicle. Human T-ALL cell lines were cultured as described in Supplemental Experimental Procedures. Cells were then stained as described above and analyzed by flow cytometry.

Human T-ALL Xenografts

KOPTK1 and DND41 cells were stably transduced with the FUW-Luc-mCherry-puro lentivirus (Kimbrel et al., 2009) to generate KOPTK1-Luc^{+} and DND41-Luc^{+} cells. To establish orthotopic xenografts, 2 × 10^{6} engineered cells were injected intravenously via the lateral tail vein into NOD-SCID-*IL2Rγ^{null}* (NSG) mice. Bioluminescence imaging was performed by injecting mice with 75 mg/kg of D-Luciferin (Promega, Madison, WI), followed by imaging on an IVIS Spectrum (Caliper Life Sciences, Hopkinton, MA). Total body bioluminescence was determined by quantifying photon flux through standardized regions of interest using the Living Images software package (Caliper Life Sciences). Mice with established disease, defined by increasing bioluminescence, were entered onto treatment with either PD 0332991 150 mg/kg by gastric gavage, or vehicle 10 ml/kg by gastric gavage. Mice were imaged at the indicated time points, and were sacrificed when they showed signs of distress.

Statistical Calculations

Statistical significance was calculated by log rank (Mantel-Cox) test for the survival curves and two-way ANOVA test for the bioluminescence data.

All other p values were calculated by Student's unpaired t test.

ACCESSION NUMBERS

Expression data can be found at http://www.ncbi.nlm.nih.gov/geo/ under superseries accession number GSE40514.

SUPPLEMENTAL INFORMATION

Supplemental Information includes seven figures, four tables, and Supplemental Experimental Procedures and can be found with this article online at http://dx.doi.org/10.1016/j.ccr.2012.09.015.

ACKNOWLEDGMENTS

We thank Drs. K. Kozar for initial help with gene-targeting constructs; E. Sicinska, Y. Geng, L. Anders, and Q. Yu for reagents, advice, and expertise. P.H. was partly supported by a fellowship from the Swedish Wennergren Foundations. This work was supported by NIH Grants R01 CA083688 and P01 CA080111 to P.S., P01 CA109901 to A.T.L., H.v.B., and P.S., and Claudia Adams Barr grant to X.L. P.S. is a consultant and a recipient of a research grant from Novartis. T.S. is supported by grants from the National Cancer Institute (1K99CA157951), the William Lawrence and Blanche Hughes Foundation, the Children's Leukemia Research Association, and the Japan Society for the Promotion of Science.

Received: January 7, 2012
Revised: June 24, 2012
Accepted: September 18, 2012
Published: October 15, 2012

REFERENCES

Anders, L., Ke, N., Hydbring, P., Choi, Y.J., Widlund, H.R., Chick, J.M., Zhai, H., Vidal, M., Gygi, S.P., Braun, P., and Sicinski, P. (2011). A systematic screen for CDK4/6 substrates links FOXM1 phosphorylation to senescence suppression in cancer cells. Cancer Cell *20*, 620–634.

Beroukhim, R., Mermel, C.H., Porter, D., Wei, G., Raychaudhuri, S., Donovan, J., Barretina, J., Boehm, J.S., Dobson, J., Urashima, M., et al. (2010). The landscape of somatic copy-number alteration across human cancers. Nature *463*, 899–905.

Bodrug, S.E., Warner, B.J., Bath, M.L., Lindeman, G.J., Harris, A.W., and Adams, J.M. (1994). Cyclin D1 transgene impedes lymphocyte maturation and collaborates in lymphomagenesis with the myc gene. EMBO J. *13*, 2124–2130.

Bowe, D.B., Kenney, N.J., Adereth, Y., and Maroulakou, I.G. (2002). Suppression of Neu-induced mammary tumor growth in cyclin D1 deficient mice is compensated for by cyclin E. Oncogene *21*, 291–298.

Burns, K.H., Agno, J.E., Sicinski, P., and Matzuk, M.M. (2003). Cyclin D2 and p27 are tissue-specific regulators of tumorigenesis in inhibin alpha knockout mice. Mol. Endocrinol. *17*, 2053–2069.

Chaganti, R.S., and Houldsworth, J. (2000). Genetics and biology of adult human male germ cell tumors. Cancer Res. *60*, 1475–1482.

Chen, D., Pacal, M., Wenzel, P., Knoepfler, P.S., Leone, G., and Bremner, R. (2009). Division and apoptosis of E2f-deficient retinal progenitors. Nature *462*, 925–929.

Chiang, M.Y., Xu, M.L., Histen, G., Shestova, O., Roy, M., Nam, Y., Blacklow, S.C., Sacks, D.B., Pear, W.S., and Aster, J.C. (2006). Identification of a conserved negative regulatory sequence that influences the leukemogenic activity of NOTCH1. Mol. Cell. Biol. *26*, 6261–6271.

Chicas, A., Wang, X., Zhang, C., McCurrach, M., Zhao, Z., Mert, O., Dickins, R.A., Narita, M., Zhang, M., and Lowe, S.W. (2010). Dissecting the unique role of the retinoblastoma tumor suppressor during cellular senescence. Cancer Cell *17*, 376–387.

Chong, J.L., Wenzel, P.L., Sáenz-Robles, M.T., Nair, V., Ferrey, A., Hagan, J.P., Gomez, Y.M., Sharma, N., Chen, H.Z., Ouseph, M., et al. (2009). E2f1-3 switch from activators in progenitor cells to repressors in differentiating cells. Nature *462*, 930–934.

Cooper, A.B., Sawai, C.M., Sicinska, E., Powers, S.E., Sicinski, P., Clark, M.R., and Aifantis, I. (2006). A unique function for cyclin D3 in early B cell development. Nat. Immunol. *7*, 489–497.

Dean, J.L., Thangavel, C., McClendon, A.K., Reed, C.A., and Knudsen, E.S. (2010). Therapeutic CDK4/6 inhibition in breast cancer: key mechanisms of response and failure. Oncogene *29*, 4018–4032.

Deshpande, A., Sicinski, P., and Hinds, P.W. (2005). Cyclins and CDKs in development and cancer: a perspective. Oncogene *24*, 2909–2915.

Fantl, V., Stamp, G., Andrews, A., Rosewell, I., and Dickson, C. (1995). Mice lacking cyclin D1 are small and show defects in eye and mammary gland development. Genes Dev. *9*, 2364–2372.

Fry, D.W., Harvey, P.J., Keller, P.R., Elliott, W.L., Meade, M., Trachet, E., Albassam, M., Zheng, X., Leopold, W.R., Pryer, N.K., and Toogood, P.L. (2004). Specific inhibition of cyclin-dependent kinase 4/6 by PD 0332991 and associated antitumor activity in human tumor xenografts. Mol. Cancer Ther. *3*, 1427–1438.

Fu, M., Wang, C., Li, Z., Sakamaki, T., and Pestell, R.G. (2004). Minireview: cyclin D1: normal and abnormal functions. Endocrinology *145*, 5439–5447.

Hayashi, S., and McMahon, A.P. (2002). Efficient recombination in diverse tissues by a tamoxifen-inducible form of Cre: a tool for temporally regulated gene activation/inactivation in the mouse. Dev. Biol. *244*, 305–318.

Hu, M.G., Deshpande, A., Enos, M., Mao, D., Hinds, E.A., Hu, G.F., Chang, R., Guo, Z., Dose, M., Mao, C., et al. (2009). A requirement for cyclin-dependent kinase 6 in thymocyte development and tumorigenesis. Cancer Res. *69*, 810–818.

Hulit, J., Wang, C., Li, Z., Albanese, C., Rao, M., Di Vizio, D., Shah, S., Byers, S.W., Mahmood, R., Augenlicht, L.H., et al. (2004). Cyclin D1 genetic heterozygosity regulates colonic epithelial cell differentiation and tumor number in ApcMin mice. Mol. Cell. Biol. *24*, 7598–7611.

Ianari, A., Natale, T., Calo, E., Ferretti, E., Alesse, E., Screpanti, I., Haigis, K., Gulino, A., and Lees, J.A. (2009). Proapoptotic function of the retinoblastoma tumor suppressor protein. Cancer Cell *15*, 184–194.

Kimbrel, E.A., Davis, T.N., Bradner, J.E., and Kung, A.L. (2009). In vivo pharmacodynamic imaging of proteasome inhibition. Mol. Imaging *8*, 140–147.

Kühn, R., Schwenk, F., Aguet, M., and Rajewsky, K. (1995). Inducible gene targeting in mice. Science *269*, 1427–1429.

Kuilman, T., and Peeper, D.S. (2009). Senescence-messaging secretome: SMS-ing cellular stress. Nat. Rev. Cancer *9*, 81–94.

Landis, M.W., Pawlyk, B.S., Li, T., Sicinski, P., and Hinds, P.W. (2006). Cyclin D1-dependent kinase activity in murine development and mammary tumorigenesis. Cancer Cell *9*, 13–22.

Li, S.K., Smith, D.K., Leung, W.Y., Cheung, A.M., Lam, E.W., Dimri, G.P., and Yao, K.-M. (2008a). FoxM1c counteracts oxidative stress-induced senescence and stimulates Bmi-1 expression. J. Biol. Chem. *283*, 16545–16553.

Li, X., Gounari, F., Protopopov, A., Khazaie, K., and von Boehmer, H. (2008b). Oncogenesis of T-ALL and nonmalignant consequences of overexpressing intracellular NOTCH1. J. Exp. Med. *205*, 2851–2861.

Lin, Y., Bloodgood, B.L., Hauser, J.L., Lapan, A.D., Koon, A.C., Kim, T.K., Hu, L.S., Malik, A.N., and Greenberg, M.E. (2008). Activity-dependent regulation of inhibitory synapse development by Npas4. Nature *455*, 1198–1204.

Lovec, H., Grzeschiczek, A., Kowalski, M.B., and Möröy, T. (1994). Cyclin D1/bcl-1 cooperates with myc genes in the generation of B-cell lymphoma in transgenic mice. EMBO J. *13*, 3487–3495.

Malumbres, M., and Barbacid, M. (2009). Cell cycle, CDKs and cancer: a changing paradigm. Nat. Rev. Cancer *9*, 153–166.

Muller, W.J., Sinn, E., Pattengale, P.K., Wallace, R., and Leder, P. (1988). Single-step induction of mammary adenocarcinoma in transgenic mice bearing the activated c-Neu oncogene. Cell *54*, 105–115.

Musgrove, E.A., Caldon, C.E., Barraclough, J., Stone, A., and Sutherland, R.L. (2011). Cyclin D as a therapeutic target in cancer. Nat. Rev. Cancer *11*, 558–572.

Narita, M., Nũnez, S., Heard, E., Narita, M., Lin, A.W., Hearn, S.A., Spector, D.L., Hannon, G.J., and Lowe, S.W. (2003). Rb-mediated heterochromatin formation and silencing of E2F target genes during cellular senescence. Cell *113*, 703–716.

O'Neil, J., Grim, J., Strack, P., Rao, S., Tibbitts, D., Winter, C., Hardwick, J., Welcker, M., Meijerink, J.P., Pieters, R., et al. (2007). FBW7 mutations in leukemic cells mediate NOTCH pathway activation and resistance to gamma-secretase inhibitors. J. Exp. Med. *204*, 1813–1824.

Park, H.J., Carr, J.R., Wang, Z., Nogueira, V., Hay, N., Tyner, A.L., Lau, L.F., Costa, R.H., and Raychaudhuri, P. (2009). FoxM1, a critical regulator of oxidative stress during oncogenesis. EMBO J. *28*, 2908–2918.

Puyol, M., Martín, A., Dubus, P., Mulero, F., Pizcueta, P., Khan, G., Guerra, C., Santamaría, D., and Barbacid, M. (2010). A synthetic lethal interaction between K-Ras oncogenes and Cdk4 unveils a therapeutic strategy for non-small cell lung carcinoma. Cancer Cell *18*, 63–73.

Reddy, H.K., Mettus, R.V., Rane, S.G., Graña, X., Litvin, J., and Reddy, E.P. (2005). Cyclin-dependent kinase 4 expression is essential for Neu-induced breast tumorigenesis. Cancer Res. *65*, 10174–10178.

Robles, A.I., Rodriguez-Puebla, M.L., Glick, A.B., Trempus, C., Hansen, L., Sicinski, P., Tennant, R.W., Weinberg, R.A., Yuspa, S.H., and Conti, C.J. (1998). Reduced skin tumor development in cyclin D1-deficient mice highlights the oncogenic ras pathway in vivo. Genes Dev. *12*, 2469–2474.

Ruas, M., Gregory, F., Jones, R., Poolman, R., Starborg, M., Rowe, J., Brookes, S., and Peters, G. (2007). CDK4 and CDK6 delay senescence by kinase-dependent and p16INK4a-independent mechanisms. Mol. Cell. Biol. *27*, 4273–4282.

Sage, J., Miller, A.L., Pérez-Mancera, P.A., Wysocki, J.M., and Jacks, T. (2003). Acute mutation of retinoblastoma gene function is sufficient for cell cycle re-entry. Nature *424*, 223–228.

Sherr, C.J., and Roberts, J.M. (2004). Living with or without cyclins and cyclin-dependent kinases. Genes Dev. *18*, 2699–2711.

Sicinska, E., Aifantis, I., Le Cam, L., Swat, W., Borowski, C., Yu, Q., Ferrando, A.A., Levin, S.D., Geng, Y., von Boehmer, H., and Sicinski, P. (2003). Requirement for cyclin D3 in lymphocyte development and T cell leukemias. Cancer Cell *4*, 451–461.

Sicinska, E., Lee, Y.M., Gits, J., Shigematsu, H., Yu, Q., Rebel, V.I., Geng, Y., Marshall, C.J., Akashi, K., Dorfman, D.M., et al. (2006). Essential role for cyclin D3 in granulocyte colony-stimulating factor-driven expansion of neutrophil granulocytes. Mol. Cell. Biol. *26*, 8052–8060.

Sicinski, P., Donaher, J.L., Parker, S.B., Li, T., Fazeli, A., Gardner, H., Haslam, S.Z., Bronson, R.T., Elledge, S.J., and Weinberg, R.A. (1995). Cyclin D1 provides a link between development and oncogenesis in the retina and breast. Cell *82*, 621–630.

Trimarchi, J.M., and Lees, J.A. (2002). Sibling rivalry in the E2F family. Nat. Rev. Mol. Cell Biol. *3*, 11–20.

Tsikitis, M., Zhang, Z., Edelman, W., Zagzag, D., and Kalpana, G.V. (2005). Genetic ablation of Cyclin D1 abrogates genesis of rhabdoid tumors resulting from Ini1 loss. Proc. Natl. Acad. Sci. USA *102*, 12129–12134.

Wang, T.C., Cardiff, R.D., Zukerberg, L., Lees, E., Arnold, A., and Schmidt, E.V. (1994). Mammary hyperplasia and carcinoma in MMTV-cyclin D1 transgenic mice. Nature *369*, 669–671.

Weng, A.P., Ferrando, A.A., Lee, W., Morris, J.P., 4th, Silverman, L.B., Sanchez-Irizarry, C., Blacklow, S.C., Look, A.T., and Aster, J.C. (2004). Activating mutations of NOTCH1 in human T cell acute lymphoblastic leukemia. Science *306*, 269–271.

Weinstat-Saslow, D., Merino, M.J., Manrow, R.E., Lawrence, J.A., Bluth, R.F., Wittenbel, K.D., Simpson, J.F., Page, D.L., and Steeg, P.S. (1995). Overexpression of cyclin D mRNA distinguishes invasive and in situ breast carcinomas from non-malignant lesions. Nat. Med. *1*, 1257–1260.

Young, A.P., and Longmore, G.D. (2004). Differential regulation of apoptotic genes by Rb in human versus mouse cells. Oncogene *23*, 2587–2599.

Yu, Q., Geng, Y., and Sicinski, P. (2001). Specific protection against breast cancers by cyclin D1 ablation. Nature *411*, 1017–1021.

Yu, Q., Sicinska, E., Geng, Y., Ahnström, M., Zagozdzon, A., Kong, Y., Gardner, H., Kiyokawa, H., Harris, L.N., Stål, O., and Sicinski, P. (2006). Requirement for CDK4 kinase function in breast cancer. Cancer Cell *9*, 23–32.

Zhang, Q., Sakamoto, K., Liu, C., Triplett, A.A., Lin, W.C., Rui, H., and Wagner, K.U. (2011). Cyclin D3 compensates for the loss of cyclin D1 during ErbB2-induced mammary tumor initiation and progression. Cancer Res. *71*, 7513–7524.